CrystEngComm

ROYAL SOCIETY OF CHEMISTRY

PAPER

View Article Online
View Journal | View Issue

Cite this: *CrystEngComm*, 2023, **25**, 2321

The introduction of a base component to porous organic salts and their CO_2 storage capability†

Takahiro Ami,‡[a] Kouki Oka,‡[a] Keiho Tsuchiya,[a] Wataru Kosaka,[bc] Hitoshi Miyasaka[bc] and Norimitsu Tohnai*[a]

Received 27th January 2023,
Accepted 3rd March 2023

DOI: 10.1039/d3ce00086a

rsc.li/crystengcomm

Porous organic salts (**POSs**) are constructed by charge-assisted hydrogen bonding between amino and sulfonic groups, and can be used to design a variety of porous structures based on molecular design. In particular, triphenylmethylamine (**TPMA**) and aromatic sulfonic acids form robust **POSs** with a rigid diamond structure (***d*-POSs**). In this study, by replacing one of the three phenyl rings of **TPMA** with a pyrimidine ring, we succeeded in constructing a ***d*-POS** with high porosity (43.8%) and with a base component (pyrimidine) on the void surface. In addition, the weak basicity of the pyrimidine did not interfere with the formation of ***d*-POSs**. This ***d*-POS** adsorbed CO_2 over the primary air components (N_2 and O_2) and also exhibited CO_2 storage capability: It retained CO_2 at a relatively low pressure of P_e/P_0 = 0.05, and readily desorbed CO_2 below P_e/P_0 = 0.05.

Introduction

Based on molecular design, the pore size, morphology, and function of porous materials fabricated from organic molecules can be precisely and easily controlled. Therefore, these materials have been extensively investigated for gas separation applications.[1–3] Typical examples of extremely designable porous organic materials are metal–organic frameworks (**MOFs**), in which organic linkers and metal elements are connected by coordination bonds,[2,4–6] and covalent-organic frameworks (**COFs**), in which organic molecules are linked by covalent bonds.[7–10] However, the fabrication of robust porous structures such as **MOFs** and **COFs** usually requires harsh and/or complicated synthesis routes (*e.g.*, microwave, voltage application, high pressure, and high temperature), and/or the use of metal elements obtained from limited resources. On the other hand, porous materials fabricated with non-covalent bonds are prepared by simple recrystallization under ambient conditions.[11,12] In particular, all-organic porous materials constructed by hydrogen bonds are called hydrogen-bonded frameworks (**HOFs**) and are intensively investigated as one of the porous organic materials because of their high crystallinity and designability.[13] Non-covalent bonds are generally considered weaker than coordination and covalent bonds. However, hydrogen bonds between strong bases and acids, such as amines and sulfonic acids, are known as "charge-assisted hydrogen bonding", and are extremely ionic and rigid.[14] The porous structures of ammonium sulfonate salts, which are constructed *via* charge-assisted hydrogen bonding, exhibit excellent robustness and rigidity.[15–20]

We previously reported that ammonium sulfonate salts, composed of bulky **TPMA** and aromatic sulfonic acids, such as tetrahedral tetrasulfonic acid (**MTBPS**), form diamondoid porous organic salts (***d*-POSs**) (Fig. 1a).[15–20] In detail, four **TPMA** molecules and four sulfonic acid molecules form a [4 + 4] supramolecular cluster (Fig. 1a, center) by self-assembly *via* rigid charge-assisted hydrogen bonding. Subsequently, these clusters are self-assembled to form the diamond network, and the interpenetration of some of the diamond networks hierarchically results in the formation of ***d*-POSs** (Fig. 1a, right).[15] The diamond network is composed of sulfonic acid molecules and the amino groups in **TPMA**; however, it does not include the triphenylmethyl group in **TPMA**. The bulky triphenylmethyl group suppresses the number of interpenetrations of the diamond network, and therefore ***d*-POSs** generally possess a relatively higher porosity than organic porous materials that contain complete amine structures.[21] Furthermore, we previously found that the phenyl rings of **TPMA** were exposed on the void surface of ***d*-POSs**, and the introduction of halogen-

[a] *Department of Applied Chemistry and Center for Future Innovation (CFi), Graduate School of Engineering, Osaka University, Osaka 565-0871, Japan. E-mail: tohnai@chem.eng.osaka-u.ac.jp*
[b] *Institute for Materials Research, Tohoku University, Sendai 980-8577, Japan*
[c] *Department of Chemistry, Graduate School of Science, Tohoku University, Sendai 980-8578, Japan*

† Electronic supplementary information (ESI) available. CCDC 2160329. For ESI and crystallographic data in CIF or other electronic format see DOI: https://doi.org/10.1039/d3ce00086a

‡ T. A. and K. O. contributed equally to this work.

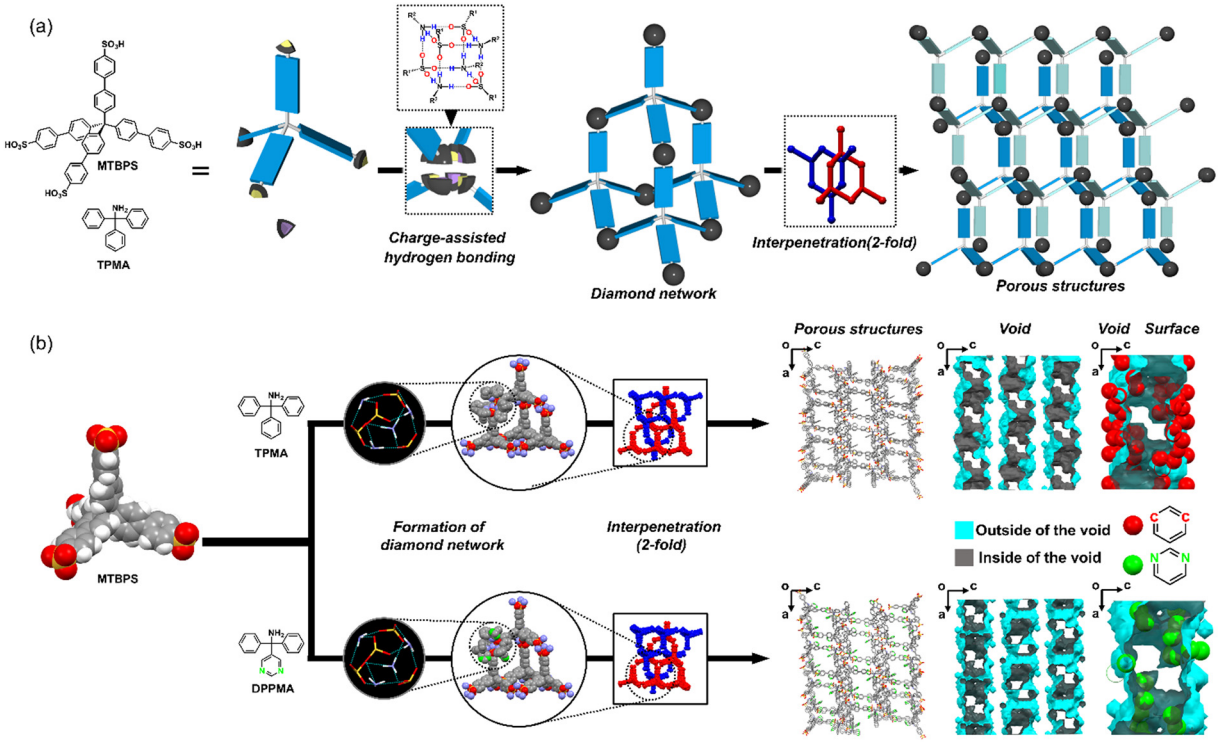

Fig. 1 Formation of diamondoid porous organic salts (***d*-POSs**) using tetrahedral tetrasulfonic acid (**MTBPS**) and triphenylmethylamine derivatives (**TPMA** or **DPPMA**). (a) Schematic images of diamond network formation from **MTBPS** and **TPMA** by charge-assisted hydrogen bonding, and of the porous structures hierarchically constructed by the interpenetration of two diamond networks. (b) Schematic image of the construction and characterization of the porous and void structures of **TPMA/MTBPS** and **DPPMA/MTBPS**.

substituents such as fluorine (F), chlorine (Cl), bromine (Br), and iodine (I) into the *para*-positions of the phenyl rings of **TPMA** enabled ***d*-POSs** to have a variety of void structures and environments. In addition, we demonstrated that their gas adsorption properties were drastically changed depending on their void structures and environments.[20]

In this study, we found that not only the *para*-positions but also *meta*-positions of the phenyl rings of **TPMA** were exposed on the void surface. Therefore, for introducing the base component into the void surface of the ***d*-POSs**, we focused on pyrimidine, which has more base components (*e.g.*, lone pair of nitrogen), and is a weaker base than primary amines. The diphenyl(pyrimidine-5-yl)methylamine (**DPPMA**) is synthesized by replacing one of the three phenyl rings of **TPMA** with a pyrimidine ring, where two nitrogen atoms are substituted at the *meta*-positions of the phenyl ring.[22] A facile recrystallization method is used to combine **DPPMA** and **MTBPS** for the fabrication of a ***d*-POS** (**DPPMA/MTBPS**) with two nitrogen atoms, with their lone pairs exposed on the void surface. In the crystal structure of DPPMA/MTBPS, the base component of the pyrimidine rings (lone pairs of the nitrogen atoms) do not interfere with the charge-assisted hydrogen bonding between amino and sulfonic groups, and therefore DPPMA/MTBPS forms a diamond network identical to that of TPMA/MTBPS. DPPMA/MTBPS adsorbed CO_2 over the primary air components (N_2 and O_2). Moreover, the adsorbed CO_2 (49.9 mL (STP)/g at P_e/P_0 = 1) was stabilized in the void *via* interactions with the pyrimidine ring.[23,24] DPPMA/MTBPS retained CO_2 down to a reasonably low pressure of P_e/P_0 = 0.05, and subsequently CO_2 was desorbed by decreasing the pressure to below P_e/P_0 = 0.05.

Experimental section

Preparation of organic salts composed of DPPMA and MTBPS

DPPMA (5 eq) and **MTBPS** (1 eq) were separately dissolved in methanol, and then mixed. After solvent evaporation, the residue was washed with diethyl ether, and the organic salts were obtained as a pale-yellow powder.

Preparation of the single-crystal of DPPMA/MTBPS.

The organic salt (2.0 mg) was recrystallized with benzonitrile (200 μL) in *N*,*N*-dimethylacetamide (400 μL) by gradually evaporating the solvent at 70 °C. The single crystals of **DPPMA/MTBPS** were obtained as colorless prisms. By repeating this process, a sufficient amount of **DPPMA/MTBPS** was collected for the gas adsorption experiments.

Results and discussion

An organic salt with an exact **TPMA : MTBPS** molecular ratio of 4 : 1 was produced by simply mixing **TPMA** and **MTBPS** in

a polar organic solvent. Subsequently, the facile recrystallization of the organic salt in *N*,*N*-dimethylformamide with 1,2,4-trichlorobenzene (a template molecule that facilitates the formation of porous structures) resulted in **TPMA/MTBPS**§ (Fig. 1b, center and S1;† for details of the preparation processes, please see the experimental section). MTBPS has a tetrahedral structure, which is consistent with the diamondoid structure, and therefore TPMA/MTBPS was selectively formed without crystal polymorphism. The single-crystal structure of TPMA/MTBPS indicated that the two diamond networks are deeply interlocked in opposite directions, forming a thermodynamically stable structure (Fig. 1b, center).

Additionally, the PLATON/VOID routine calculation showed that **TPMA/MTBPS** has a high porosity of 40.7%. After the evacuation of a template molecule using the supercritical fluid carbon dioxide process (**SCFCO$_2$**),[26] **TPMA/MTBPS** (Fig. S2a†) adsorbed CO_2 over the primary air components, such as N_2 and O_2 (Fig. S2b†). This was ascribed to the quadrupole–quadrupole interactions[27,28] between CO_2 (with a strong quadrupole moment)[29] and the phenyl rings exposed on the void surface, and the smaller kinetic diameter of CO_2 (3.30 Å[30]) than those of N_2 (3.64 Å[30]) and O_2 (3.46 Å[30]).

This study aimed to introduce the base component into the void surface of the ***d*-POSs**. In **TPMA/MTBPS**, the *para*-positions and *meta*-positions of the phenyl rings of **TPMA** are exposed on the void surface (Fig. 1b, void surface). Thus, we hypothesized that the incorporation or substitution of base functional groups at the *para*-positions or *meta*-positions of phenyl rings would introduce the base component into the void surface. Therefore, a **TPMA** derivative (**DPPMA**) was synthesized by replacing one of the phenyl rings of **TPMA** with a pyrimidine ring, where two nitrogen atoms and their lone pairs were substituted at the *meta*-positions of the phenyl ring. Nitrogen atoms and their lone pairs on the pyrimidine ring are known showing weak basicity.[23,24] Subsequently, by combining **DPPMA** with **MTBPS**, **DPPMA/MTBPS** similar to **TPMA/MTBPS** (Fig. 1b, right and S3;† for details of the synthesis processes, please see the experimental section) was successfully prepared. Notably, the single-crystal X-ray structure analysis revealed that the base component (lone pairs of the nitrogen atoms) of the pyrimidine ring do not interfere with the charge-assisted hydrogen bonding between the amino and sulfonic groups. **DPPMA/MTBPS** forms a diamond network identical to that of **TPMA/MTBPS** (Fig. 1b, right and S4†). This indicates that pyrimidine is less likely to interact with the sulfonic acid than with the amino group of **TPMA** because of the weaker basicity of pyrimidine than primary amines.[31,32] The porosity of **DPPMA/MTBPS** is exhibited a slightly higher porosity of 43.8% compared to that of **TPMA/MTBPS** (Table S2†), because the replacement of the phenyl ring with a pyrimidine ring increases the void volume owing to the loss of the hydrogen atoms. Additionally, the porosity of **DPPMA/MTBPS** is the highest in the other reported ***d*-POSs**[15,16,18,20] and organic porous structures with diamond networks (Table S3†).[33–36] Thermogravimetric analysis (**TGA**) data (Fig. S5†) and the number of electrons found in the masking routine revealed that the crystals of **DPPMA/MTBPS** immediately following formation *via* crystallization included six *N*,*N*-dimethylacetamide molecules and three benzonitrile molecules per one **MTBPS** molecule and four **DPPMA** molecules, which were equivalent to 29.5% of total weight. Furthermore, as designed, the nitrogen atoms and their lone pairs on the pyrimidine rings are exposed on the void surface of **DPPMA/MTBPS** (Fig. 1b, right), and, per unit cell, 48 nitrogen atoms are exposed on the void surface. It is noteworthy that changing the *meta*-positions of the phenyl rings of **TPMA** successfully tuned the void environment, while maintaining the void shape of **TPMA/MTBPS**. Variable temperature powder X-ray diffraction (**VT-PXRD**) (Fig. S6†) of **DPPMA/MTBPS** revealed that the porous structure of **DPPMA/MTBPS** was maintained up to approximately 100 °C. Furthermore, **DPPMA/MTBPS** shows high stability for nonpolar solvents such as diethyl ether and benzene. However, the crystallinity of **DPPMA/MTBPS** was decreased after soaking in the polar solvents, water, and acidic/basic aqueous solutions (Fig. S7†), presumably because of the partial dissolution of DPPMA/MTBPS. Similar to TPMA/MTBPS, the template molecule in DPPMA/MTBPS was evacuated by $SCFCO_2$ while maintaining the porous structure (Fig. 2a and S8†).

The gas adsorption properties of **DPPMA/MTBPS**, after the evacuation of the template molecule, for CO_2, N_2, and O_2 were evaluated. The **PXRD** patterns of **TPMA/MTBPS** and **DPPMA/MTBPS** did not change before and after the sorption experiments (Fig. S9†). Therefore, these **POSs** maintained their porous structures after the sorption experiments, and their gas adsorption behavior is highly reproducible even after the second time. **DPPMA/MTBPS** adsorbed 49.9 mL (STP)/g of CO_2 at P_e/P_0 = 1.0, 2.87 mL (STP)/g of N_2 at P_e/P_0 = 0.97, and 1.07 mL (STP)/g of O_2 at P_e/P_0 = 0.99 (Fig. 2b). **DPPMA/MTBPS** exhibited the same selective adsorption behavior for CO_2 as that of **TPMA/MTBPS**. In addition, the CO_2 adsorption isotherm revealed that DPPMA/MTBPS had a CO_2-BET surface area of 192 $m^2\ g^{-1}$ (Table S2†) and an average pore size of 10.2 Å (Fig. S10†). On the other hand, DPPMA/MTBPS did not adsorb N_2 and O_2, therefore the pore size distribution analysis based on the N_2 and O_2 adsorption isotherms were unable to be performed. The large hysteresis observed in the CO_2 adsorption/desorption behavior of DPPMA/MTBPS demonstrates that CO_2 is retained on the void surface by interactions with the pyrimidine rings. DPPMA/MTBPS retains the CO_2 adsorbed at P_e/P_0 = 1.0 when the pressure is decreased to P_e/P_0 = 0.05 (Fig. 2b and S11†), whereas TPMA/MTBPS releases approximately 50% of the adsorbed CO_2 (Fig. S2b†). Furthermore, the strength of

§ The crystal structure of **TPMA/MTBPS** has been reported in our previous work.[20] Deposition Number 2160329 (**DPPMA/MTBPS**) contain the supplementary crystallographic data for this paper.

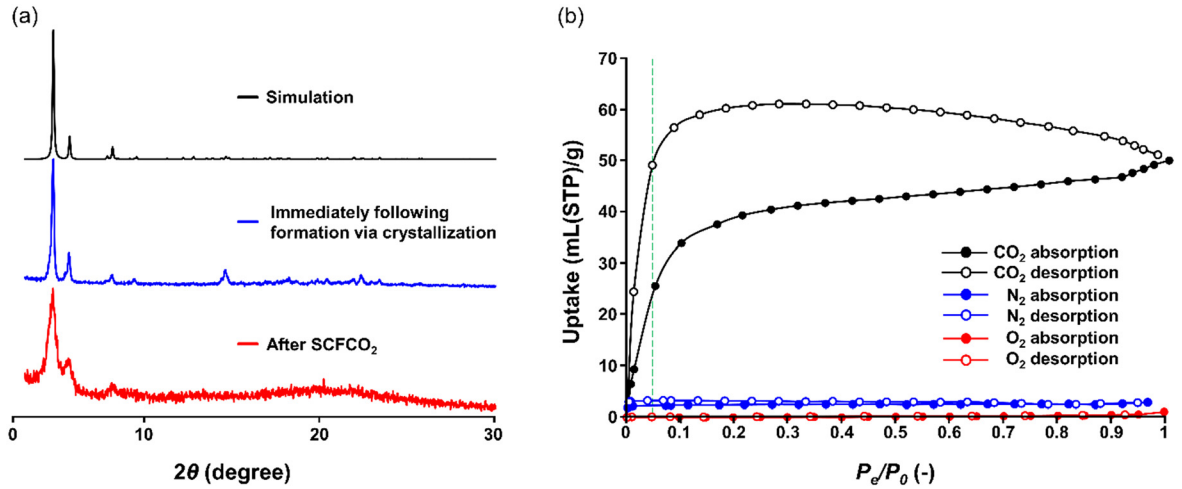

Fig. 2 Characterization of the diamondoid porous organic salts (**DPPMA/MTBPS**). (a) Powder X-ray diffraction (**PXRD**) patterns of **DPPMA/MTBPS**, simulation (black), immediately following formation *via* crystallization (blue), after conducting the supercritical fluid carbon dioxide (**SCFCO$_2$**) process for 5 h (red). (b) Gas adsorption/desorption isotherms of **DPPMA/MTBPS** in the cases of nitrogen (N_2, 77 K), oxygen (O_2, 77 K), and carbon dioxide (CO_2, 195 K). P_e denotes the pressure at gas adsorption and P_0 is the condensation pressure of the adsorbate at the measurement temperature. Green line is P_e/P_0 = 0.05. The amount of CO_2 adsorption of **DPPMA/MTBPS** reaches a maximum value at P_e/P_0 = 0.2 in the desorption isotherm which is common in porous structures with complicated micropores such as **MOFs** because of the extremely slow diffusion rate of the adsorbent in their void.[25]

interactions between pyrimidine or phenyl rings and CO_2 molecules was evaluated by Fourier transform infrared (FT-IR) spectroscopy measurements under CO_2 atmospheres. However, as shown in Fig. S12,† no significant differences were found between the spectra measured under vacuum and CO_2 atmospheres. This means that these interactions are weaker than the general chemical interactions. Therefore, although DPPMA/MTBPS retains CO_2 up to P_e/P_0 = 0.05, it can readily desorb the adsorbed CO_2 below P_e/P_0 = 0.05. The ability to retain CO_2 over a wide pressure range (0.05–1.0 atm) may play a very important role in CO_2 storage and utilization processes.[37]

Conclusions

In this study, **DPPMA**, where two nitrogen atoms and their lone pairs are substituted at the *meta*-positions of the phenyl ring, and **MTBPS** were combined to form ***d*-POSs**. The pyrimidine ring did not interfere with the charge-assisted hydrogen bonding between the sulfonic and primary amino groups, and therefore **DPPMA/MTBPS** formed the same crystal structure as that of **TPMA/MTBPS**. Furthermore, as designed, the nitrogen atoms and their lone pairs on the pyrimidine rings were exposed on the void surface of **DPPMA/MTBPS**, and the base components were successfully introduced into the void surface while maintaining the void shape of **TPMA/MTBPS**. **DPPMA/MTBPS** adsorbed CO_2 over the primary air components (N_2 and O_2), which was ascribed to strong quadrupole–quadrupole interactions with the phenyl rings on the void surface. **DPPMA/MTBPS** retained the adsorbed CO_2 in the void down to a reasonably low pressure of P_e/P_0 = 0.05 (originally adsorbed at P_e/P_0 = 1.0), which was attributed to interactions between the pyrimidine rings and CO_2. Moreover, when the pressure was decreased to below P_e/P_0 = 0.05, **DPPMA/MTBPS** readily desorbed the adsorbed CO_2. Therefore, **DPPMA/MTBPS** captured and retained CO_2 even at a relatively low CO_2 pressure of 0.08–0.13 atm, which is comparable to that of a waste incinerator,[38] or 0.05 atm, which is comparable to that of a natural gas combined cycle power station.[39] Therefore, the introduction of a functional component (even a base component) into the benzene rings of **TPMA** enables the void environment and the functionalities of **POSs** to be precisely designed.

Author contributions

Takahiro Ami and Kouki Oka contributed equally to this work. Takahiro Ami: conceptualization, methodology, formal analysis, data curation, investigation, and writing – original draft. Kouki Oka: conceptualization, methodology, formal analysis, data curation, project administration, validation, supervision, investigation, and writing – original draft. Keiho Tsuchiya: investigation. Wataru Kosaka: investigation and writing – review & editing. Hitoshi Miyasaka: writing – review & editing. Norimitsu Tohnai: conceptualization, methodology, data curation, project administration, validation, supervision, investigation, writing – review & editing, funding acquisition, and resources.

Conflicts of interest

The authors declare no conflict of interest.

Acknowledgements

This work was partially supported by Grants-in-Aids for Scientific Research (20H00381, 20H02548, 21K18925,

21H01900, and 22K14732) from MEXT, Japan. K. O. also acknowledges the support from LNest Grant from Nipponham, FUSO Innovative Technology Fund, Masuyakinen basic research foundation, and Shorai Foundation for Science and Technology.

Notes and references

1 Q. Qian, P. A. Asinger, M. J. Lee, G. Han, K. Mizrahi Rodriguez, S. Lin, F. M. Benedetti, A. X. Wu, W. S. Chi and Z. P. Smith, *Chem. Rev.*, 2020, **120**, 8161–8266.
2 R.-B. Lin, S. Xiang, W. Zhou and B. Chen, *Chem*, 2020, **6**, 337–363.
3 L. Zhu and Y.-B. Zhang, *Molecules*, 2017, **22**, 1149.
4 S. Zhou, Z. Qiu, M. Strømme and C. Xu, *Energy Environ. Sci.*, 2021, **14**, 900–905.
5 J. K. Zareba, M. Nyk and M. Samoc, *Cryst. Growth Des.*, 2016, **16**, 6419–6425.
6 O. M. Yaghi, M. O'Keeffe, N. W. Ockwig, H. K. Chae, M. Eddaoudi and J. Kim, *Nature*, 2003, **423**, 705–714.
7 K. Oka, B. Winther-Jensen and H. Nishide, *Adv. Energy Mater.*, 2021, **11**, 2003724.
8 K. Geng, T. He, R. Liu, S. Dalapati, K. T. Tan, Z. Li, S. Tao, Y. Gong, Q. Jiang and D. Jiang, *Chem. Rev.*, 2020, **120**, 8814–8933.
9 C. S. Diercks and O. M. Yaghi, *Science*, 2017, **355**, 923.
10 A. P. Cote, A. I. Benin, N. W. Ockwig, M. O'Keeffe, A. J. Matzger and O. M. Yaghi, *Science*, 2005, **310**, 1166–1170.
11 R.-B. Lin, Y. He, P. Li, H. Wang, W. Zhou and B. Chen, *Chem. Soc. Rev.*, 2019, **48**, 1362–1389.
12 J. Luo, J.-W. Wang, J.-H. Zhang, S. Lai and D.-C. Zhong, *CrystEngComm*, 2018, **20**, 5884–5898.
13 I. Hisaki, C. Xin, K. Takahashi and T. Nakamura, *Angew. Chem., Int. Ed.*, 2019, **58**, 11160–11170.
14 P. Gilli, L. Pretto, V. Bertolasi and G. Gilli, *Acc. Chem. Res.*, 2009, **42**, 33–44.
15 A. Yamamoto, S. Uehara, T. Hamada, M. Miyata, I. Hisaki and N. Tohnai, *Cryst. Growth Des.*, 2012, **12**, 4600–4606.
16 A. Yamamoto, T. Hamada, I. Hisaki, M. Miyata and N. Tohnai, *Angew. Chem., Int. Ed.*, 2013, **52**, 1709–1712.
17 A. Yamamoto, T. Hasegawa, T. Hamada, T. Hirukawa, I. Hisaki, M. Miyata and N. Tohnai, *Chem. – Eur. J.*, 2013, **19**, 3006–3016.
18 A. Yamamoto, T. Hirukawa, I. Hisaki, M. Miyata and N. Tohnai, *Tetrahedron Lett.*, 2013, **54**, 1268–1273.
19 T. Miyano, N. Okada, R. Nishida, A. Yamamoto, I. Hisaki and N. Tohnai, *Chem. – Eur. J.*, 2016, **22**, 15430–15436.
20 T. Ami, K. Oka, K. Tsuchiya and N. Tohnai, *Angew. Chem.*, 2022, **134**, e20222597.
21 S. Yu, G. L. Xing, L. H. Chen, T. Ben and B. L. Su, *Adv. Mater.*, 2020, **32**, 2003270.
22 M. Berthelot, C. Laurence, M. Safar and F. Besseau, *J. Chem. Soc., Perkin Trans. 2*, 1998, 283–290.
23 K. D. Vogiatzis, A. Mavrandonakis, W. Klopper and G. E. Froudakis, *ChemPhysChem*, 2009, **10**, 374–383.
24 I. Kaljurand, T. Rodima, I. Leito, I. A. Koppel and R. Schwesinger, *J. Org. Chem.*, 2000, **65**, 6202–6208.
25 J. Ethiraj, S. Palla and H. Reinsch, *Microporous Mesoporous Mater.*, 2020, **294**, 109867.
26 J. E. Mondloch, O. Karagiaridi, O. K. Farha and J. T. Hupp, *CrystEngComm*, 2013, **15**, 9258–9264.
27 J. H. Williams, *Acc. Chem. Res.*, 1993, **26**, 593–598.
28 S. K. Valzita, *Chem. Phys. Lett.*, 1981, **78**, 421–423.
29 J. R. Li, R. J. Kuppler and H. C. Zhou, *Chem. Soc. Rev.*, 2009, **38**, 1477–1504.
30 B. Freeman, Y. Yampolskii and I. Pinnau, *Materials science of membranes for gas and vapor separation*, John Wiley & Sons Ltd., West Sussex, 2006.
31 T. P. Selvam, C. R. James, P. V. Dniandev and S. K. Valzita, *J. Res. Pharm.*, 2015, **2**, 1–9.
32 I. Juranić, *Croat. Chem. Acta*, 2014, **87**, 343–347.
33 H. Kim and M. P. Suh, *Inorg. Chem.*, 2005, **44**, 810–812.
34 K. M. E. Jones, A. H. Mahmoudkhani, B. D. Chandler and G. K. H. Shimizu, *CrystEngComm*, 2006, **8**, 303–305.
35 P. Metrangolo, F. Meyer, T. Pilati, D. M. Proserpio and G. Resnati, *Chem. – Eur. J.*, 2007, **13**, 5765–5772.
36 D. Beaudoin, T. Maris and J. D. Wuest, *Nat. Chem.*, 2013, **5**, 830–834.
37 R. E. Morris and P. S. Wheatley, *Angew. Chem., Int. Ed.*, 2008, **47**, 4966–4981.
38 H. Lee, S.-M. Yi, T. M. Holsen, Y.-S. Seo and E. Choi, *Waste Manage.*, 2018, **73**, 247–255.
39 J.-M. G. Amann and C. Bouallou, *Energy Procedia*, 2009, **1**, 909–916.